6. Geochemical Cycling of Fluorine, Chlorine, Bromine, and Boron and Implications for Fluid-Rock Reactions in Mariana Forearc, South Chamorro Seamount, ODP Leg 195[1]

Wei Wei[2], Miriam Kastner[2], Annette Deyhle[2],
and Arthur J. Spivack[3]

ABSTRACT

At the South Chamorro Seamount in the Mariana subduction zone, geochemical data of pore fluids recovered from Ocean Drilling Program Leg 195 Site 1200 indicate that these fluids evolved from dehydration of the underthrusting Pacific plate and upwelling of fluids to the surface through serpentinite mud volcanoes as cold springs at their summits. Physical conditions of the fluid source at 27 km were inferred to be at 100°–250°C and 0.8 GPa. The upwelling of fluid is more active near the spring in Holes 1200E and 1200A and becomes less so with increasing distance toward Hole 1200D. These pore fluids are depleted in Cl and Br, enriched in F (except in Hole 1200D) and B (up to 3500 µM), have low $\delta^{11}B$ (16‰–21‰), and have lower than seawater Br/Cl ratios. The mixing ratios between seawater and pore fluids is calculated to be ~2:1 at shallow depth. The F, Cl, and Br concentrations, together with B concentrations and B isotope ratios in the serpentinized igneous rocks and serpentine muds that include ultramafic clasts from Holes 1200A, 1200B, 1200D, 1200E, and 1200F, support the conclusion that the fluids involved in serpentinization originated from great depths; the dehydration of sediments and altered basalt at the top of the subducting Pacific plate released Cl, H_2O, and B with enriched ^{10}B. Calculation from B concentrations and upwelling rates indicate that B is efficiently recycled

through this nonaccretionary subduction zone, as through others, and may contribute the critical missing B of the oceanic cycle.

INTRODUCTION

Fluid production and transport affect the thermal regime of convergent margins, metamorphism in the suprasubduction zone region, diagenesis in forearc sediments, biological activity, and, ultimately, the composition of arc and backarc magmas.

Cold (~2°C) springs of fluid with salinity lower than seawater have been found in several mud volcanoes in the Mariana intraoceanic subduction complex between the northwestward subducting Pacific plate and the overriding Philippine plate. Volatiles released from the downgoing Pacific plate hydrate the overlying mantle wedge and convert depleted harzburgite to low-density serpentinite. The resulting serpentinite mud, containing variably serpentinized harzburgite clasts, ascends buoyantly along fractures and extrudes at the seafloor, where it forms large (30 km diameter, 2 km high) mud volcanoes along the outer Mariana forearc in a band that extends from 50 to 120 km behind the trench axis (Fryer, 1992; Fryer et al. 1985, 1995, 2000).

Relative to seawater, the deep upwelling fluids in South Chamorro Seamount (Leg 195) and Conical Seamount (Leg 125) have higher to much higher sulfate, alkalinity, K, Rb, B, light hydrocarbons, and ammonium concentrations; higher pH, Na/Cl, $\delta^{18}O$, and δD values; and lower to much lower chloride, Mg, Ca, Sr, Li, Si, and phosphate concentrations and Sr isotopic ratios (Benton, 1997; Benton et al., 2001; Mottl, 1992; Mottl et al., 2003). By contrast, pore fluids from inactive Torishima Forearc Seamount (Leg 125) show different behaviors for these geochemical tracers, purportedly produced by reaction of cold seawater with harzburgite (Mottl, 1992). Therefore, the deeply sourced upwelling fluids within the two active serpentine mud volcanoes clearly cannot have originated by simple reaction of seawater with peridotite, but rather by dehydration of sediments and altered basalt at the top of the subducting Pacific plate (Fryer et al., 1999; Mottl et al., 2003).

The South Chamorro Seamount F, Cl, Br, and B concentrations and B isotopes are discussed below. They add new insights to previous studies of the Mariana forearc region (Benton, 1997; Benton et al., 2001; Savov et al., 2004) on the geochemical cycling, fluid production and transport, and origin of probably the most pristine slab-derived fluids recovered from a subduction zone.

Halogens are excellent tracers of fluids during subduction because their geochemical behavior is dominated by strong partitioning into the fluid phase. Chloride, Br, and F substitutions in minerals typically involve sites occupied chiefly by hydroxyl ions and, as such, are at least partly covalently bonded in the crystal structure. Therefore, it has been predicted that Cl, Br, and F exchange will be a sensitive function of fluid pH (Zhu, 1993). Temperature is also influencing the halogen exchange dynamics. The large size differences between the hydroxyl ions, fluoride, chloride, and bromide suggest that their relative exchange should also be sensitively affected by pressure (Vanko, 1986). B isotope fractionation between solids and fluids is thought to relate to the preferential incorporation of ^{10}B-rich $B(OH)_4$ into silicate minerals. Thus, it is strongly influenced by pH and temperature as well (Spivack et al., 1987; You et al., 1996; Palmer et al., 1998; Sanyal et al., 2000). B isotope

ratios and concentrations may provide evidence for serpentine formation and clay alteration at depth (Spivack et al., 1987; Palmer, 1996; Deyhle et al., 2001; Deyhle and Kopf, 2001, 2002; Benton et al., 2001). When serpentine forms, B uptake is high and isotope ratios ($^{11}B/^{10}B$) in the residual solution increase (Bonatti et al., 1984; Spivack and Edmond, 1987; Benton et al., 2001) because of preferential uptake of ^{10}B by solids. The adsorption of B also occurs at low temperature, and the adsorbed species is predominantly the light isotope ^{10}B as well (Spivack et al., 1987; Palmer and Swihart, 1996). In general, at greater depths and thus increasing temperature and pressure, B enriches in fluids by processes such as release of adsorbed B from clays, mineral dehydration reactions, possible release of structurally bound B, and alteration of volcanic rocks (Seyfried et al., 1984; Spivack et al., 1987; You et al., 1996; Palmer and Swihart, 1996, Deyhle and Kopf, 2001, 2002).

GEOLOGICAL BACKGROUND

The South Chamorro Seamount drilled during Leg 195 is located on the southern Mariana forearc in the nonaccretionary convergent margin west of the Mariana Trench (Fig. F1). Site 1200 is at the summit of the seamount ~85 km from the trench (Salisbury, Shinohara, Richter, et al., 2002). At several sites, slab-derived fluids and muds that consist mostly of serpentine and blueschist metamorphosed minerals are venting from a depth of ~27 km (Fryer, 1996; Maekawa et al., 1993) to form very large (30 km diameter, 2 km high) mud volcanoes with long-lived conduits (Fryer, 1992). Medium blue-green to dark blue serpentine mud and clasts of metamorphosed rocks are exposed, and fissure seeps support an active biological community (Fryer and Mottl, 1992). Brucite and carbonate chimneys were also observed and possibly are a surface manifestation of decarbonation reactions.

Hole 1200E is located within 10 m of Hole 1200A, and a seep was identified by the presence of mussels, small tubeworms, and galatheid crabs. Hole 1200B is ~20 m east of Holes 1200A and 1200E. Holes 1200F and 1200D are ~20 and 80 m north of Hole 1200E, respectively, and thus constitute a transect northward from the seep (Fig. F2). Temperature gradients estimated from Holes 1200E and 1200F are 0.0092°C/m and 0.0724°C/m, respectively, such that none of the interstitial water exceeded 3.0°C at the sampling depth, compared with a bottom-water temperature of 1.67°C (Shipboard Scientific Party, 2002).

ANALYTICAL METHODS

Chemical Concentrations in Fluids

At Scripps Institute of Oceanography, F, Br, and SO_4 concentrations were analyzed by ion chromatography (IC) with a precision of 3%. B concentration was analyzed by inductively coupled plasma–optical emission spectrometer (ICP-OES) with a typical relative standard deviation of 1%–5%. The samples were reanalyzed for Cl by the $AgNO_3$ titration method to check for possible evaporation (precision = 0.1%).

F1. Seamount locations, p. 15.
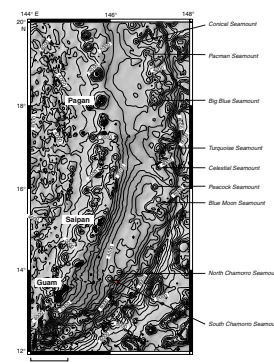
F2. Drill hole locations, p. 16.
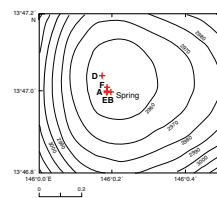
Mineralogy

X-ray diffraction (XRD) was used to determine sample mineralogy, in particular to identify hydrous silicate phases. Some of the hydrous phases (i.e., serpentine and brucite) were physically separated using classical methods that are based on grain size and density. The purity of the mineral separates was also examined by scanning electron microscopy. The identification of serpentine forms (chrysotile, lizardite, and antigorite) is being pursued.

Halogens, Sulfur, and Boron in Solids

Volatiles such as halogens (F, Cl, and Br) were extracted from silicates by the pyrohydrolysis method (Dreibus et al., 1979) as modified in Scripps laboratories (Magenheim et al., 1994). Pyrohydrolysis results in the quantitative removal of volatiles from silicates, thereby eliminating extraction-induced isotopic artifacts (Magenheim et al., 1994). The extracted fluids were analyzed for anion concentrations (F, Cl, Br, and SO_4^{2-}) on IC with a precision of 3%.

Boron was extracted from solids by HF digestion and numerous ion exchanges in the presence of mannitol in order to suppress loss of B (Nakano and Nakamura, 1998; Deyhle, 2001). Concentrations were determined by ICP-OES.

Isotopic Analyses

Fluorine has no naturally occurring isotopes. Because of the unusually high pH (~12) and alkalinity (70–100 mM) in the pore fluids from Mariana (Salisbury, Shinohara, Richter, et al., 2002; Mottl et al., 2003), routine chemical preparation procedures for analysis of Cl isotopes by mass spectrometry were not appropriate. The high CO_3^{2-} and OH^- concentrations in the samples interfered with the Cs_2Cl^+ signal during ionization in the mass spectrometer. Thus, only samples with close to seawater pH values have produced reliable results. Development of a new sample preparation method is in progress. Therefore, in this report, the stable isotopic work is focused on B for both fluid and solid samples.

Boron isotope ratios in solids were determined by positive thermal ionization mass spectrometry (P-TIMS, Finnigan MAT 262, at GEOMAR, Kiel, Germany). This TIMS is equipped with a static double collector system, specifically designed to analyze Cs_2BO^+ masses 308 and 309 simultaneously. By repeatedly analyzing the boric acid National Bureau of Standards standard reference material (NBS SRM) 951 as well as rock standard JB-2 and other silicatic samples, the external reproducibility of natural samples was determined to be ±0.11‰–0.16‰ for analyses for 100 ng B loaded on a Ta filament (Deyhle, 2001). The internal precision of samples measured for this study varied between 0.02‰ and 0.06‰ (Table T1).

Boron isotope ratios in pore fluid were determined by negative thermal ionization mass spectrometry, following the procedure outlined in Zuleger and Erzinger (1991) and Deyhle et al. (2001). In order to obtain stable BO_2^- signals, 0.5 µL of B-free seawater matrix was loaded onto Re zone-refined filaments together with 1 µL of sample. External precision is ±0.5‰ ($2\sigma_{mean}$), and average internal precision is 0.05‰. B concentration and isotopes in fluids were corrected because of possible pH,

temperature, and pressure changes during sample recovery on the drill-ship, following suggestions of You et al. (1996). The corrections reduce the B concentrations between 7% and 10%, but B isotopic results are not affected by the corrections, which are within the range of the external precision.

RESULTS

Pore Fluid Chemistry

The concentrations of chloride in the pore fluids from all sites are lower than in bottom seawater by as much as 7% (Table T1; Fig. F3). Interestingly, the Cl concentrations measured were not as low as those observed at Conical Seamount.

Bromide concentration-depth profiles are similar to those of Cl (Fig. F3A, F3C). The values are also lower than the seawater value and exhibit a steep depletion in concentration within the uppermost 4.5 meters below seafloor (mbsf); deeper they remain approximately constant. The Br profile in Hole 1200F has the typical convex-upward shape and steep near-surface gradient, indicative of upwelling at 1–10 cm/yr (Mottl et al., 2003). The profiles of Br/Cl ratios with depth (Fig. F3D) show that at shallow depths the Br/Cl ratios in Holes 1200E and 1200F decrease with depth at a much sharper gradient than in Hole 1200D; at greater depths, the ratio values from Holes 1200A, 1200D, and 1200E converge to ~1.40–1.45. The Br/Cl vs. 1/Cl plot from all Site 1200 holes (Fig. F4) shows a straight line, indicating mixing between the end-member ascending fluid and bottom seawater. All 1/Cl values are higher than that of seawater because of Cl depletion with depth. Br/Cl values from shallow depths of Hole 1200D and seafloor samples of Holes 1200E and 1200F are higher than seawater Br/Cl, whereas the deeper Br/Cl values are lower than the seawater value. This implies that Br is more depleted than Cl in the source fluid (see "Discussion," p. 7). In general, Br/Cl ratios in Hole 1200D are higher than in Holes 1200E, 1200F, and 1200A (Fig. F3D, F4) because Hole 1200D is farther away from the spring and upwelling is slower. This evolution phenomenon along the transect of holes (Fig. F2) is shown by other geochemical profiles, such as K (Mottl et al., 2003).

Fluoride concentrations in pore fluids were determined on board (Shipboard Scientific Party, 2002). Generally, our IC results show similar trends to those obtained from the ion selective electrode method (Fig. F3C; Table T1). In Hole 1200D, the farthest from the spring, fluoride concentrations decrease sharply within the uppermost meter below the seafloor, from 68 µM to almost 0 µM and then rebound to ~50 µM at 30 mbsf. At the spring and close to it in Hole 1200E, fluoride first increases to ~110 µM above 20 mbsf then decreases to 50 µM at greater depth. In Hole 1200F, fluoride concentration is ~40 µM at the seafloor and increases to ~80 µM with depth. F/Cl vs. depth profiles (Fig. F3E) indicate that at shallow depths (<20 mbsf), the values in Holes 1200E and 1200F are higher than in seawater, whereas in Hole 1200D, F/Cl ratios are much lower. At greater depth (>20 mbsf), F/Cl ratios merge to the seawater value, with the deepest sample in Hole 1200A having greater than seawater value, implying that F and Cl released by the solids have slightly higher F/Cl ratios than seawater.

Boron concentrations in pore fluids increase sharply from 416 to ~3500 µM immediately within 5 mbsf and remain constant with depth

F3. Pore fluid profiles, p. 17.
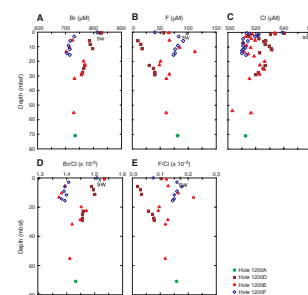
F4. Br/Cl vs. 1/Cl in pore fluids, p. 18.
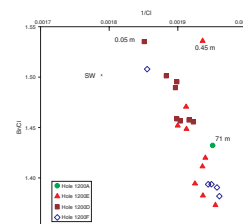
to the deepest uncontaminated sample at 70 mbsf (Fig. F5A, F5B). Boron values in pore fluids are high (~3600 μM) compared with the seawater value of 416 μM. Concentration gradients based on our analysis of Hole 1200E samples are steeper (Fig. F5A) than those of Hole 1200D (Mottl et al., 2003), also implying that upwelling is stronger closer to the spring. B/Cl ratios at depth (Fig. F5A) are about six times seawater value, indicating that the upwelling fluids are greatly enriched in B. The high B concentration is also observed in the pore fluid data set from Conical Seamount (Mottl, 1992; Benton, 1997; Benton et al., 2001).

Pore Fluid Isotope Data

Because of the problems encountered with the preparation method for Cl isotopic analysis (discussed above), these data are not presented here and will be discussed elsewhere.

Boron isotope signatures in the pore fluids are significantly depleted relative to the seawater value of 39.5‰ (Spivack and Edmond, 1987) (Fig. F5C; Table T1). They are reported as $\delta^{11}B$ in permil deviation from the standard (SRM 951 boric acid) as follows: $\delta^{11}B = 1000$ $(^{11}B/^{10}B_{sample}/^{11}B/^{10}B_{standard} - 1)$. Even the pore fluid sample from closest to the seafloor in Section 195-1200E-1H-1 has a value of 20‰, much lower than the seawater value of 39.5‰. $\delta^{11}B$ values gradually decrease with depth to 16‰ at 71 mbsf. The gradient is higher at shallower depths (from 21‰ to 17‰ at 0.95–15 mbsf, then 16‰ at 15–71 mbsf). The crossplot of $\delta^{11}B$ vs. 1/B (Fig. F6) shows that $\delta^{11}B$ evolves from the lowest value of 16‰ in the deepest sample to 20‰ in the shallowest sample, having relatively constant but much higher (~3–8 times) than seawater B concentration throughout the depth range analyzed. This implies mixing even at the shallow depth. Provided the sample (1500 μM B with $\delta^{11}B = 21.5‰$) at 1 mbsf is a mixture of seawater (416 μM B with $\delta^{11}B = 39.5‰$) and upwelling fluids (3500 μM B with $\delta^{11}B = 16‰$), the calculation shows that the seawater accounts for ~65% and the upwelling fluid for ~35% at 1 mbsf, while below 5 mbsf, upwelling fluid constitutes more than 99% of the fluid analyzed.

Sample Description and Bulk Solid Mineralogy

The only solid analyzed from Hole 1200A is a highly altered igneous basement sample and the one from Hole 1200B is only partially altered to serpentine with relics of the primary mineral matrix of clionopyroxene, orthopyroxene, and olivine. All the solids analyzed from Hole 1200D, 1200E, and 1200F are highly altered serpentine muds. XRD analysis of the bulk samples shows that the major mineral is serpentine (Table T2). Brucite, calcite, and aragonite are also present in the samples from Holes 1200A, 1200D, and 1200E (Table T2). Brucite most probably coprecipitated due to the high pH. Aragonite needles have precipitated abundantly within the upper 2 mbsf of both active mud volcanoes, where plentiful Ca is supplied by downward diffusion from seawater (Mottl, 1992; Shipboard Scientific Party, 2002). Other trace minerals detected by XRD are chlorite, amphibole, and talc and are shown in Table T2.
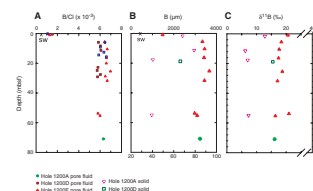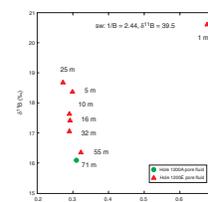
Bulk Solid Chemistry

Chlorine concentrations in bulk solids vary between holes (Table T2). The highest concentration (~650 ppm) is in Hole 1200B at 33.2 mbsf. In Hole 1200A, Cl in bulk solids is ~480 ppm at 18.8 mbsf. In Hole 1200F, it increases from 280 ppm at 0 mbsf to 430 ppm at 8.2 mbsf. The depth profiles (Fig. F7) show that the Cl concentrations in Holes 1200F, 1200A, and 1200B increase with depth. In Holes 1200D and 1200E, the data show a different pattern of slightly decreasing Cl concentrations with depth. In Hole 1200E, Cl content in bulk solids slightly decreases from 200 to 120 ppm with depth, whereas in Hole 1200D, bulk Cl content is in the range of 80 to 150 ppm. The Cl concentration range could be due to lithologic difference (altered igneous basement vs. serpentine muds) or forms of serpentines (lizardite, chrysotile, or antigorite) because lizardite and chrysotile contain more Cl than antigorite (Scambelluri et al., 2004). This suggests that due to the denser structure of antigorite, Cl may behave as an incompatible element and, thus is unable to be retained in antigorite as tightly as in lizardite or chrysotile.

All bulk solid samples contain <100 ppm F, except at depths of 10 to 15 mbsf in Hole 1200E, F is enriched up to 400 ppm (Table T2). XRD analysis of this solid sample (Section 195-1200E-3H-1) has shown that it contains ~40% aragonite. A fluoride peak is also observed in the corresponding pore fluid sample. No Br was detected in any of the solids by IC method; therefore, Br is not shown in the table. Sulfur is also detected in solids (Table T2). The S depth profile (Fig. F7) shows that S is enriched in near-surface solid samples, due to Fe sulfide precipitation (Mottl et al., 2003).

Solid Isotope Data

In Hole 1200E, B concentrations in solids (Table T2; Fig. F5B) are ~70–80 ppm (up to twice the pore fluid value of 1.4 to 3.6 mM [~16–39 ppm]) in the upper 10 mbsf and decrease sharply to a constant concentration of ~40 ppm (slightly higher than the pore fluid value of 3.5 mM, [38.5 ppm]) below ~10 mbsf. The B isotope value is 13‰ in the surface sample and decreases to 7‰ at depth (Fig. F5C). In Hole 1200A, the solid sample from 18.8 mbsf shows B concentration of ~66 ppm and isotopic ratio of 15.5‰; higher than at the equivalent depth in Hole 1200E (Fig. F5C). High heterogeneity and different mineral composition might have an influence on differences in B contents and isotope values.

DISCUSSION

The geochemical results of higher to much higher sulfate, alkalinity, K, Rb, B, light hydrocarbons, and ammonium concentrations; higher pH, Na/Cl, $\delta^{18}O$ and δD values; lower to much lower chloride, Mg, Ca, Sr, Li, Si, phosphate concentrations and Sr isotopic ratios; and also lower Ba, Mn, Fe, and bisulfide concentrations than seawater values (Shipboard Scientific Party, 2002; Mottl et al., 2003) indicate that there are two major processes taking place in South Chamorro Seamount: upwelling of a fluid from a deep source and microbial sulfate reduction near the seafloor. Both processes are more enhanced in Hole 1200E near the spring and become less so with increasing distance toward Holes
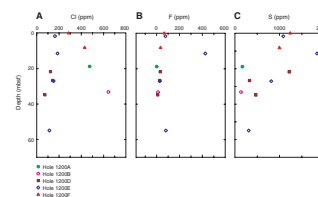
1200A and 1200D, as indicated by all geochemical profiles (Mottl et al., 2003). Our data show that these fluids have lower than seawater Br/Cl and $\delta^{11}B$ values but are enriched in B concentrations. Fluoride concentrations and F/Cl show different trends between Hole 1200D and Holes 1200E and 1200F, probably due to coprecipitation with carbonates. These data support the conclusion that the fluid originates from greater depth, where dehydration of sediments and altered basalt at the top of the subducting Pacific plate occurs, thus releasing F, Cl, and B with enriched ^{10}B relative to seawater, and H_2O, in which F/Cl ratios are slightly higher than seawater value (Fig. F3E) and Cl concentrations are lower than seawater value (Fig. F3C). The mixing of these fluids with seawater at shallow depth is indicated by Br and B concentrations as well as B isotopes, and mixing ratios between seawater and pore fluids are ~2:1 at shallow depth (<5 mbsf).

Bromide has a larger radius than F and Cl, which may retard its substitution for OH^- sites in the hydrous minerals. Thus, solids preferentially uptake F and Cl instead of Br. This is further proven by the Br/Cl values shown in Figures F3D and F4 in the deeper pore fluids of Holes 1200A, 1200E, and 1200F. When the solids dehydrate, the water is released as well as Cl and F, but not Br. Thus pore fluids have lower Br/Cl ratios than the seawater value of 1.5 (Fig. F4). Figure F4 also shows that Br/Cl is progressively becoming lower from Hole 1200D (farther from the spring) to 1200E and 1200F (closer to the spring). The Cl concentration in the dehydrated fluids is lower than seawater value; therefore, although Cl is being released, Cl concentration is still lower than seawater and becomes less so near the spring (Fig. F4). In contrast, in the Nankai subduction zone, where high-temperature reactions occur (≥250°C), Cl is taken up by the solids but Br is not; therefore, Br/Cl ratios in pore fluids are ~1.8, higher than that in seawater (Wei et al., 2003). The opposite trends in the Br/Cl ratios observed at Mariana forearcs vs. Nankai subduction zone are likely caused by reactions (hydration vs. dehydration) at the different pressure, temperature, and pH and involving different types of subducting sediments at the two subduction systems.

The B concentrations and isotopic variation in the serpentinites from South Chamorro Seamount (39–79 ppm B, $\delta^{11}B$ = 6.2‰–12.8‰ in serpentine muds; 66.18 ppm, $\delta^{11}B$ = 15.49‰ in highly altered igneous rock) (Table T2) show variations like those reported by Benton et al., (2001) from the Conical Seamount (6–126 ppm B, $\delta^{11}B$ = 11‰–20.6‰ in serpentine matrix; 6.8–57.5 ppm B, $\delta^{11}B$ = 5.4‰–25.3‰ in clasts). Lower B concentrations were reported by Savov et al. (this volume) (1.1–28.5 ppm for serpentine muds; 10.8–60.8 ppm for schists) and Snyder et al. (this volume) (7–19 ppm for serpentine muds; 18–32 ppm for schists). Savov et al. (2004) also report a range of $\delta^{11}B$ isotopes (10.6‰–14.3‰) in serpentinized ultramafic rocks, which is closer to our results. Only a few data on B in serpentinite are available in the literature; Spivack and Edmond (1987) report B contents from 81 ppm to 50 ppm, with B isotopic signatures between 8.3‰ and 12.5‰ in samples from the Vema Fracture Zone in the equatorial Atlantic. Smith et al. (1995) also show highly variable B results for oceanic crust from Deep Sea Drilling Program and ODP holes (1.1–104 ppm, –4.3‰–24.9‰; south of the Bermuda Rise). Thus, a potential explanation for the observed range of reported B data from Leg 195 can be the highly heterogeneous character of the serpentine samples, ranging from highly altered oceanic crust to serpentine chlorite schists (for detailed

description see Table T1). Furthermore, different samples were analyzed in the different studies, and thus direct comparison is difficult. In addition, a recent intercomparison on B analyses (Gonfiantini et al., 2003) implies that care must be taken regarding the choice of method for analysis of B contents and $\delta^{11}B$ isotopes because of potentially varying results (Gonfiantini et al., 2003). Benton et al. (2001) and our study applied HF digestion for B extraction on the muds; **Snyder et al.** (this volume) and **Savov et al.** (this volume) applied Na_2CO_3 flux fusion in Pt crucibles. Whether differences in B contents are partially method-dependent or chiefly dependent on heterogeneity of samples analyzed is beyond the scope of this study. However, this problem needs further attention in the B community, and was already addressed by Gonfiantini et al. (2003). Nevertheless, the discussion is not influenced by the above-mentioned different data sets.

The B signatures in the solids are a result of chemical exchange with upwelling pore fluids containing ~3600 µM B (Mottl, 1992; Benton et al., 2001) (Fig. F5). It is inferred from the $\delta^{11}B$ of the solids that the upwelling slab fluid has a $\delta^{11}B$ of about 13‰ (Benton et al., 2001), representing the lower limit of $\delta^{11}B$ in pore fluids, because the high pH of the pore fluids should minimize fluid-mineral isotopic fractionation. As B speciation in solution is strongly dependent on pH, at pH ~12, essentially 100% of pore fluid B will be speciated as tetrahedral $B(OH)_4^-$. The measured $\delta^{11}B$ in the upwelling pore fluids at South Chamorro Seamount is ~16‰ (Fig. F5C), somewhat higher than the 13‰ value estimated by Benton et al. (2001). However, these are the lowest $\delta^{11}B$ signatures ever reported in ODP subduction zone fluids.

The B contents and isotopes of pore fluids indicate that the fluid source is from the subducted Pacific slab, which contains marine sediments ($\delta^{11}B$ = –17‰ to +4.8‰) (Ishikawa and Nakamura, 1993) and altered oceanic crust ($\delta^{11}B$ = +0.1‰ to +9.2‰) (Spivack and Edmond, 1987). The slab could release B with $\delta^{11}B$ of ~16‰ in two ways: desorption or dehydration of hydrous minerals. Desorbable B from solids has a $\delta^{11}B$ of 14‰ to 16‰ (N = 6) (Spivack et al., 1987) and a nondesorbable fraction that is structurally bound B in solids (85% of the B inventory in subducting sediments) has a $\delta^{11}B$ of –4‰ to +3‰ (Spivack et al., 1987).

As indicated by other geochemical tracers, dehydration of minerals must be occurring at depth during subduction (Mottl et al., 2003). The $\delta^{11}B$ difference between B in pore fluids (16‰) and structurally bound B in subducted sediments ranges from 13‰ to 20‰. Peacock and Hervig (1999) have shown that subduction-zone metamorphic rocks have a $\delta^{11}B$ value of –11‰ to +3‰, decreasing $\delta^{11}B$ of the subducting solids by as much as 14‰. This suggests that slab dehydration reactions significantly lower the $\delta^{11}B$ values of subducted oceanic crust and sediments and enrich the pore fluid in ^{11}B. Boron isotopic fractionation is higher at relatively low temperatures, and steady-state thermal models suggest physical conditions of the fluid source at 27 km to be at 100°–250°C and 0.8 Gpa (e.g., Peacock, 1996; Kincaid and Sacks, 1997). The high pH (~12) in upwelling pore fluids would also minimize fluid-mineral isotopic fractionation (Mottl et al., 2003).

IMPLICATIONS FOR GEOCHEMICAL CYCLING

The cycling of volatiles in subduction zones is Earth's deepest hydrologic cycle, with profound impact on global budgets of volatiles, gov-

erning the composition of the ocean and atmosphere, arc and backarc volcanoes, and mantle.

As shown in the pore fluids at Site 1200, Cl, as well as F and water, is released from serpentinites by metamorphic dehydration reactions during deep subduction. Serpentinite may thus provide a particularly effective fertile volatile and water source for fluid reflux through both mud volcanoes and the mantle. A 15% serpentinized peridotite will deliver into the subduction zone 4%–6% bound water, which is 2–5 times the water content of wet mafic oceanic crust (Peacock, 1990). Even 1% volume fraction of serpentine would be a significant source of water delivered to the mantle. However, in order to calculate the Cl cycling, Cl isotopic ratios in both pore fluids and serpentinites are required and will be discussed elsewhere.

Boron concentration in seawater has been nearly constant over the past 21 m.y. (Spivack et al., 1993). This implies that there is also a close balance of inputs and outputs for B (Spivack et al., 1993). The proposed outputs of B in the ocean are uptake during low-temperature weathering of the oceanic crust, adsorption on clastic sediments, and coprecipitation in carbonates (Spivack et al., 1987) and the inputs are rivers, hydrothermal vents, and fluid expelled from accretionary prisms in subduction zones (Lemarchand et al., 2000). The data from Mariana forearc show that the fluids from nonaccretionary prisms also contribute significantly to the B cycle. The estimates of B budgets indicate that the output flux (2.5×10^{10} mol/yr) is far more than the input flux (0.6×10^{10} mol/yr) (Spivack et al., 1987; Smith et al., 1995; Vengosh et al., 1991). Based on the data from Nankai, You et al. (1993) suggested that the fluids expelled from Earth's subduction process contributes 0.2×10^{10} mol/yr as reflux, balancing only 10% of the seawater budget. The most likely "missing" B input source is associated with volatilization in island-arc magma genesis, derived from subducted slab and/or sediments (You et al., 1993). The data from the Mariana subduction zone support this suggestion. The deeper fluids, which are released by dehydration and expelled by advection, are enriched in B up to 3.7 mM, with an upwelling rate of up to 10 cm/yr, which gives a B mass flux of 0.37 mol/yr/m². If the total area of the South Chamorro Seamount is 707 km² (based on a seamount diameter of 30 km), the B flux is 3×10^8 mol/yr. There are nine identified active seamounts in the Mariana forearc (Fig. F1), and there are most likely more which have not yet been identified. If we assume the identified seamounts have similar B concentrations and flux rates, as indicated by the data from Conical Seamount and South Chamorro Seamount, the total B flux is ~0.3×10^{10} mol/yr. This is only a minimum estimated fraction of the total B flux in this nonaccretionary subduction zone. Accordingly, the B reflux during plate subduction seems to be a critical part in the oceanic B cycle.

ACKNOWLEDGMENTS

REFERENCES

Benton, L.D., 1997. Origin and evolution of serpentine seamount fluids, Mariana and Izu–Bonin forearcs: implications for the recycling of subducted material [Ph.D. dissert.]. Univ. Tulsa.

Benton, L.D., Ryan, J.G., and Tera, F., 2001. Boron isotope systematics of slab fluids as inferred from a serpentine seamount, Mariana forearc. *Earth Planet. Sci. Lett.,* 187:273–282.

Bonatti, E., Lawrence, J.R., and Morandi, N., 1984. Serpentinization of ocean-floor peridotites: temperature dependence on mineralogy and boron content. *Earth Planet. Sci. Lett.,* 70:88–94.

Deyhle, A., 2001. Improvements of boron isotope analysis by positive thermal ionization mass spectrometry using static multi-collection of $Cs_2BO_2^+$ ions. *Int. J. Mass Spectrom.,* 206:79–89.

Deyhle, A., and Kopf, A., 2001. Deep fluids and ancient pore waters at the backstop: stable isotope systematics (B, C, O) of mud volcano deposits on the Mediterranean Ridge accretionary wedge. *Geology,* 29(11):1031–1034.

Deyhle, A., and Kopf, A., 2002. Strong B enrichment and anomalous $\delta^{11}B$ in pore fluids from the Japan Trench forearc. *Mar. Geol.,* 183:1–15.

Deyhle, A., Kopf, A., and Eisenhauer, A., 2001. Boron systematics of authigenic carbonates: a new approach to identify fluid processes in accretionary prisms. *Earth Planet. Sci. Lett.,* 187:191–205.

Driebus, G., Spettel, B., and Wanke, H. 1979. Halogens in meteorites and their primordial abundances. In *Origin and Distribution of the Elements* (Vol. 34): *Proceedings of the Second Symposium, Paris, France, May 10–13, 1977:* Oxford (Permagon Press), 34:33–38.

Fryer, P., 1992. A synthesis of Leg 125 drilling of serpentine seamounts on the Mariana and Izu-Bonin forearcs. *In* Fryer, P., Pearce, J.A., Stokking, L.B., et al., *Proc. ODP, Sci. Results,* 125: College Station, TX (Ocean Drilling Program), 593–614.

Fryer, P., 1996. Evolution of the Mariana convergent margin. *Rev. Geophys.,* 34:89-125.

Fryer, P., Ambos, E.L., and Hussong, D.M., 1985. Origin and emplacement of Mariana forearc seamounts. *Geology,* 13(11):774–777.

Fryer, P., Lockwood, J.P., Becker, N., Phipps, S., and Todd, C.S., 2000. Significance of serpentine mud volcanism in convergent margins. *Spec. Pap.—Geol. Soc. Am.,* 349:35–51.

Fryer, P. and Mottl, M.J., 1992. Lithology, mineralogy, and origin of serpentine muds recovered from Conical and Torishima forearc seamounts: results of Leg 125 drilling. *In* Fryer, P., Pearce, J.A., Stokking, L.B., et al., *Proc. ODP, Sci. Results,* 125: College Station, TX (Ocean Drilling Program), 343–362.

Fryer, P., Mottl, M., Johnson, L., Haggerty, J., Phipps, S., and Maekawa, H., 1995. Serpentine bodies in the forearcs of western Pacific convergent margins: origin and associated fluids. *In* Taylor, B., and Natland, J. (Eds.), *Active Margins and Marginal Basins of the Western Pacific.* Geophys. Monogr., 88:259–279.

Fryer, P., Wheat, C.G., and Mottl, M.J., 1999. Mariana blueschist mud volcanism: implications for conditions within the subduction zone. *Geology,* 27:103–106.

Gonfiantini, R., Tonarini, S., Gröning, M., Adorni-Braccesi, A., Al-Ammar, A.S., Astner, M., Bächler, S., Barnes, R.M., Bassett, R.L., Cocherie, A., Deyhle, A., Dini, A., Ferrara, G., Gaillardet, J., Grimm, J., Guerrot, C., Krähenbühl, U., Layne, G., Lemarchand, D., Meixner, A., Northington, D.J., Pennisi, M., Reitznerová, E., Rodushkin, I., Sugiura, N., Surberg, R., Tonn, S., Wiedenbeck, M., Wunderli, S., Xiao, Y., and Zack, T., 2003. Intercomparison of boron isotope and concentration measurements: Part II. Evaluation of results. *Geostand. Newsl.,* 27(1):41–57.

Ishikawa, T., and Nakamura, E., 1993. Boron isotope systematics of marine sediments. *Earth Planet. Sci. Lett.,* 117:567–580.

Kincaid, C., and Sacks, S., 1997. Thermal and dynamical evolution of the upper mantle in subduction zones. *J. Geophys. Res.,* 102:12295–12315.

Lemarchand, D., Gaillardet, J., Lewin, E., and Allegre, C., 2000. The influence of rivers on marine boron isotopes and implications for reconstructing past ocean pH. *Nature (London, U. K.),* 408(6815):951–954.

Maekawa, H., Shozuni, M., Ishii, T., Fryer, P., and Pearce, J.A., 1993. Blueschist metamorphism in an active subduction zone. *Nature (London, U. K.),* 364:520–523.

Magenheim, A.J., Spivack, A.J., Volpe, C., and Ransom, B., 1994. Precise determination of stable chlorine isotopic ratios in low-concentration natural samples. *Geochim. Cosmochim. Acta,* 58(14):3117–3121.

Mottl, M.J., 1992. Pore waters from serpentinite seamounts in the Mariana and Izu-Bonin forearcs, Leg 125: evidence for volatiles from the subducting slab. *In* Fryer, P., Pearce, J.A., Stokking, L.B., et al., *Proc. ODP, Sci. Results,* 125: College Station, TX (Ocean Drilling Program), 373–385.

Mottl, M.J., Komor, S.C., Fryer, P., and Moyer, C.L., 2003. Deep-slab fluids fuel extremophilic Archaea on a Mariana forearc serpentinite mud volcano: Ocean Drilling Program Leg 195. *Geochem., Geophys., Geosyst.,* 4:10.1029/2003GC000588.

Nakano, T., and Nakamura, E., 1998. Static multicollection of $Cs_2BO_2^+$ ions for precise boron isotope analysis with positive thermal ionization mass spectrometry. *Int. J. Mass Spectrom.,* 176:13–21.

Palmer, M.R., 1996. Hydration and uplift of the oceanic crust on the Mid-Atlantic Ridge associated with hydrothermal activity: evidence from boron isotopes. *Geophy. Res. Lett.,* 23(23):3479–3482.

Palmer, M.R., Pearson, P.N., and Cobbs, S.J., 1998. Reconstructing past ocean pH-depth profiles. *Science,* 282(5393):1468–1471.

Palmer, M.R., and Swihart, G.H., 1996. Boron isotope geochemistry: an overview. *In* Grew, E.S., and Anovitz, L.M. (Eds.), Boron: Mineralogy, Petrology and Geochemistry. *Rev. Mineral.,* 33:709–744.

Peacock, S.M., 1990. Fluid processes in subduction zones. *Science,* 248:329–337.

Peacock, S.M., 1996. Thermal and petrologic structure of subduction zones. *In* Bebout, G.E., Scholl, D.W., Kirby, S.H., and Platt, J.P. (Eds.), *Subduction Top to Bottom.* Geophys. Monogr., 96:119–133.

Peacock, S.M., and Hervig, R.L., 1999. Boron isotopic composition of subduction-zone metamorphic rocks. *Chem. Geol.,* 160(4):281–290.

Salisbury, M.H., Shinohara, M., Richter, C., et al., 2002. *Proc. ODP, Init. Repts.,* 195 [CD-ROM]. Available from: Ocean Drilling Program. Texas A&M University, College Station TX 77845-9547, USA.

Savov, I.P., Tonarini, S., Ryan, J., and Mottl, M., 2004. Boron isotope geochemistry of serpentinites and porefluids from Leg 195, Site 1200, S. Chamorro Seamount, Mariana forearc region [32nd Session of the International Geological Congress, Florence, Italy, 20–28 August 2004]. (Abstract)

Sanyal, A., Nugent, M., Reeder, R.L., and Bijma, J., 2000. Seawater pH control on the boron isotopic composition of calcite: evidence from inorganic calcite precipitation experiments. *Geochim. Cosmochim. Acta,* 64(9):1551–1555.

Scambelluri, M., Muntener, O., Ottolini, L., Pettke, T.T., and Vannucci, R., 2004. The fate of B, Cl, and Li in the subducted oceanic mantle and in the antigorite breakdown fluids. *Earth Planet. Sci. Lett.,* 222:217–234.

Seyfried, W.E., Jr., Janecky, D.R., and Mottl, M.J., 1984. Alteration of the oceanic crust: implications for geochemical cycles of lithium and boron. *Geochim. Cosmochim. Acta,* 48:557–569.

Shipboard Scientific Party, 2002. Leg 195 summary. *In* Salisbury, M.H., Shinohara, M., Richter, C., et al., *Proc. ODP, Init. Repts.,* 195: College Station TX (Ocean Drilling Program), 1–63.

Smith, H.J., Spivack, A.J., Staudigel, H., and Hart., S.R., 1995. The boron isotopic composition of altered oceanic crust. *Chem. Geol.,* 126(2):119–135.

Spivack, A.J., and Edmond, J.M., 1987. Boron isotope exchange between seawater and oceanic cust. *Geochim. Cosmochim. Acta,* 51:1033–1043.

Spivack, A.J., Palmer, M.R., and Edmond, J.M., 1987. The sedimentary cycle of the boron isotopes. *Geochim. Cosmochim. Acta,* 51:1939–1949.

Spivack, A.J., You, C.F., and Smith, H.J., 1993. Foraminiferal boron isotope ratios as a proxy for surface ocean pH over the past 21 Myr. *Nature (London, U. K.),* 363(6425):149–151.

Vanko, D.A., 1986. High-chlorine amphiboles from oceanic rocks: product of highly saline hydrothermal fluids. *Am. Mineral.,* 71:51–59.

Vengosh, A., Kolodny, Y., Starinsky, A., Chivas, A.R., and McCulloch, M.T., 1991. Coprecipitation and isotopic fractionation of boron in modern biogenic carbonates. *Geochim. Cosmochim. Acta,* 55:2901–2910.

Wei, W., Kastner, M., and Spivack, A.J., 2003. Halogen concentrations and stable isotopes (O, Sr, and Cl) in the Nankai Muroto Transect and their implication for fluid-sediment interactions and fluid flow. *Eos, Trans. Am. Geophys. Union,* 84(46):T52C-0293. (Abstract)

You, C.F., Castillo, P.R., Gieskes, J.M., Chan, L.H., and Spivack, A.J., 1996. Trace element behavior in hydrothermal experiments: implications for fluid processes in subduction zones. *Earth Planet Sci. Lett.,* 140(1–4):41–52.

You, C.-F., Spivack, A.J., Smith, J.H., and Gieskes, J.M., 1993. Mobilization of boron at convergent magins: implications for boron geochemical cycle. *Geology,* 21:207–210.

Zhu, C., 1993. New pH sensor for hydrothermal fluids. *Geology,* 21(11):983–986.

Zuleger, E., and Erzinger, J., 1991. Determination of boron isotopes using negative thermal ionization mass spectrometry, Finnigan isotope mass spectrometry. *Appl. Rept.,* 78.

Figure F1. Locations of the two active serpentinite mud volcanoes, Conical Seamount (Leg 125, Site 779) and South Chamorro Seamount (Leg 195, Site 1200) in the Mariana forearc (Fryer et al., 1999; Salisbury, Shinohara, Richter, et al., 2002).
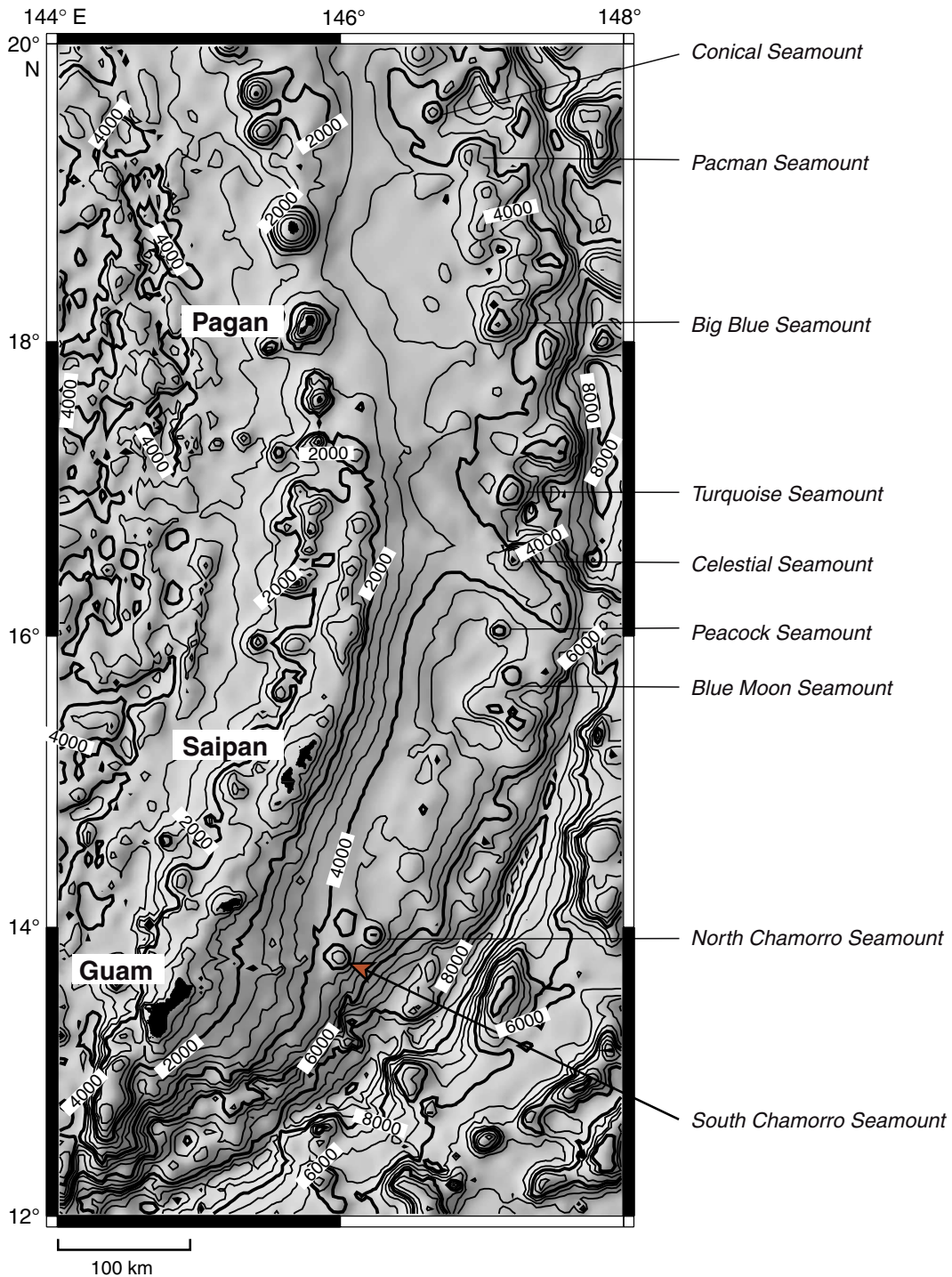
Figure F2. Positions of Site 1200 drill holes on the summit of South Chamorro Seamount. Holes 1200A and 1200E are within a few meters of an active cold spring. Depth contours are in meters. (Salisbury, Shinohara, Richter, et al., 2002).
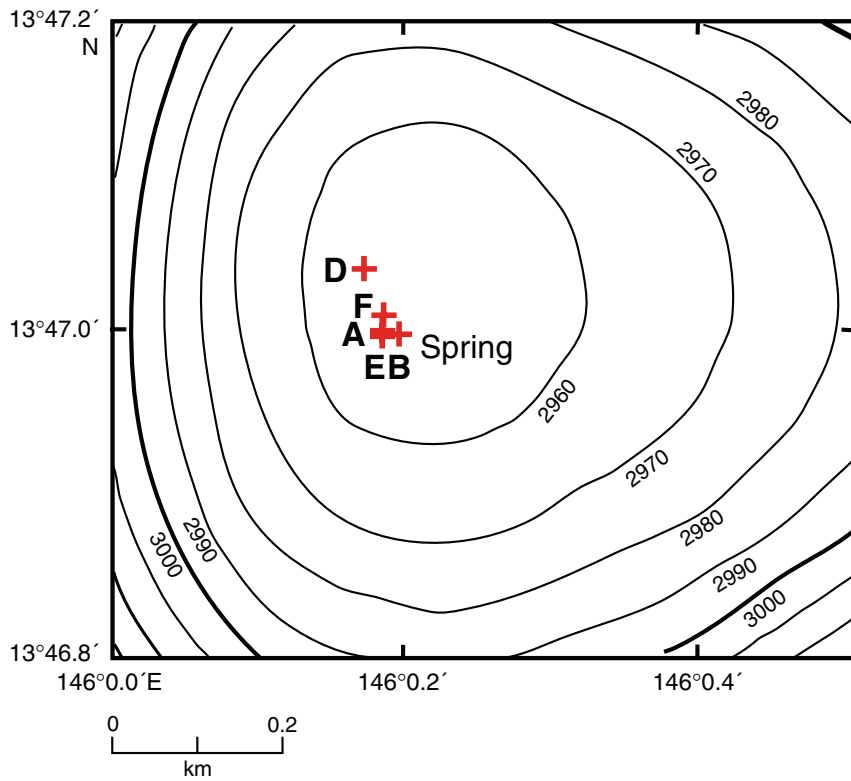
Figure F3. (**A**) Br concentration-depth, (**B**) F concentration-depth, (**C**) Cl concentration-depth, (**D**) Br/Cl concentration ratios-depth, and (**E**) F/Cl concentration ratios-depth profiles in pore fluids. Chloride was analyzed shipboard, F was analyzed both shipboard and on shore, and Br was analyzed on shore. SW= International Association for the Physical Sciences of the Ocean seawater.
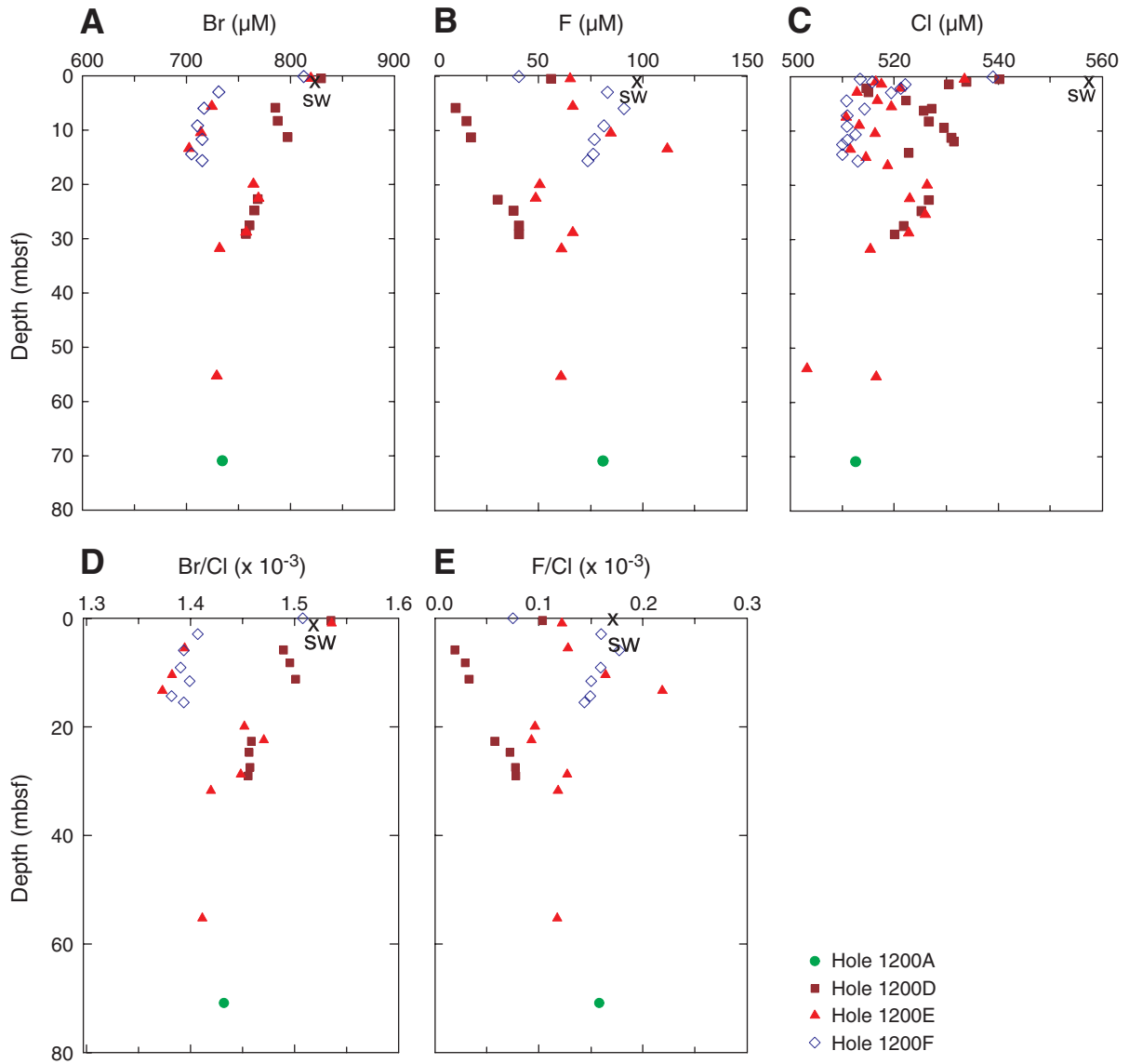
Figure F4. Br/Cl vs. 1/Cl in pore fluids. SW= International Association for the Physical Sciences of the Ocean seawater.
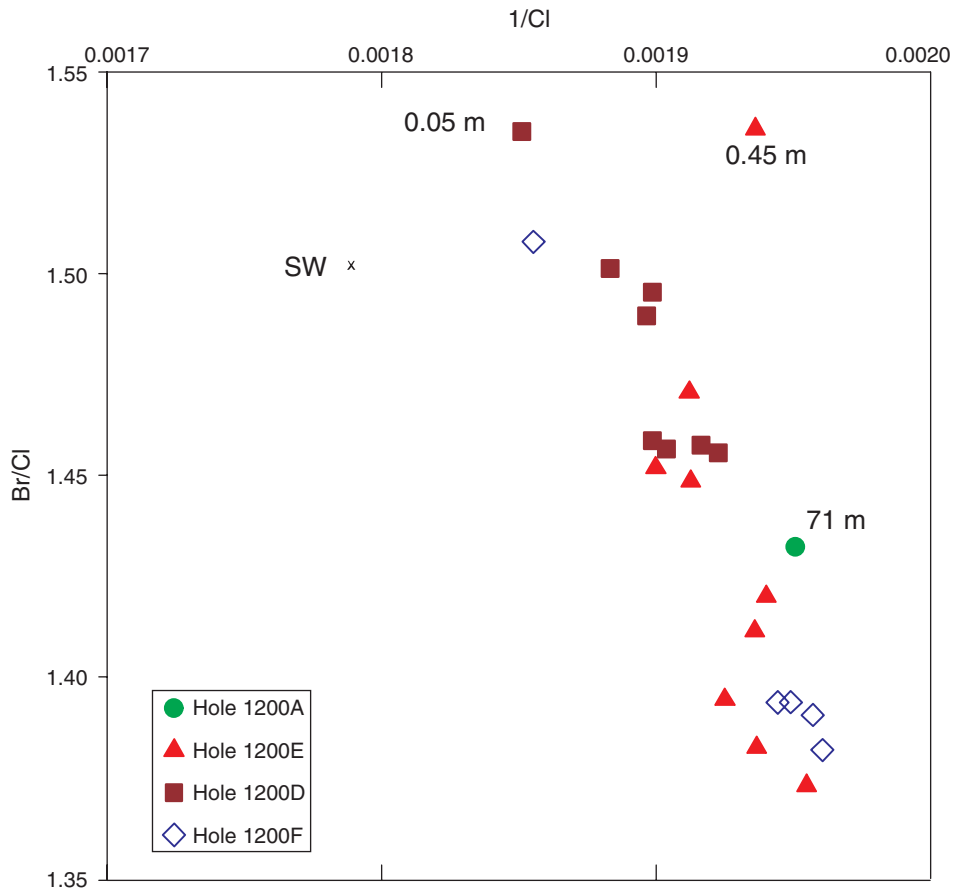
Figure F5. A. B/Cl concentration ratio-depth profiles. **B.** B concentration-depth profiles. **C.** $\delta^{11}B$-depth profiles. SW= International Association for the Physical Sciences of the Ocean seawater.
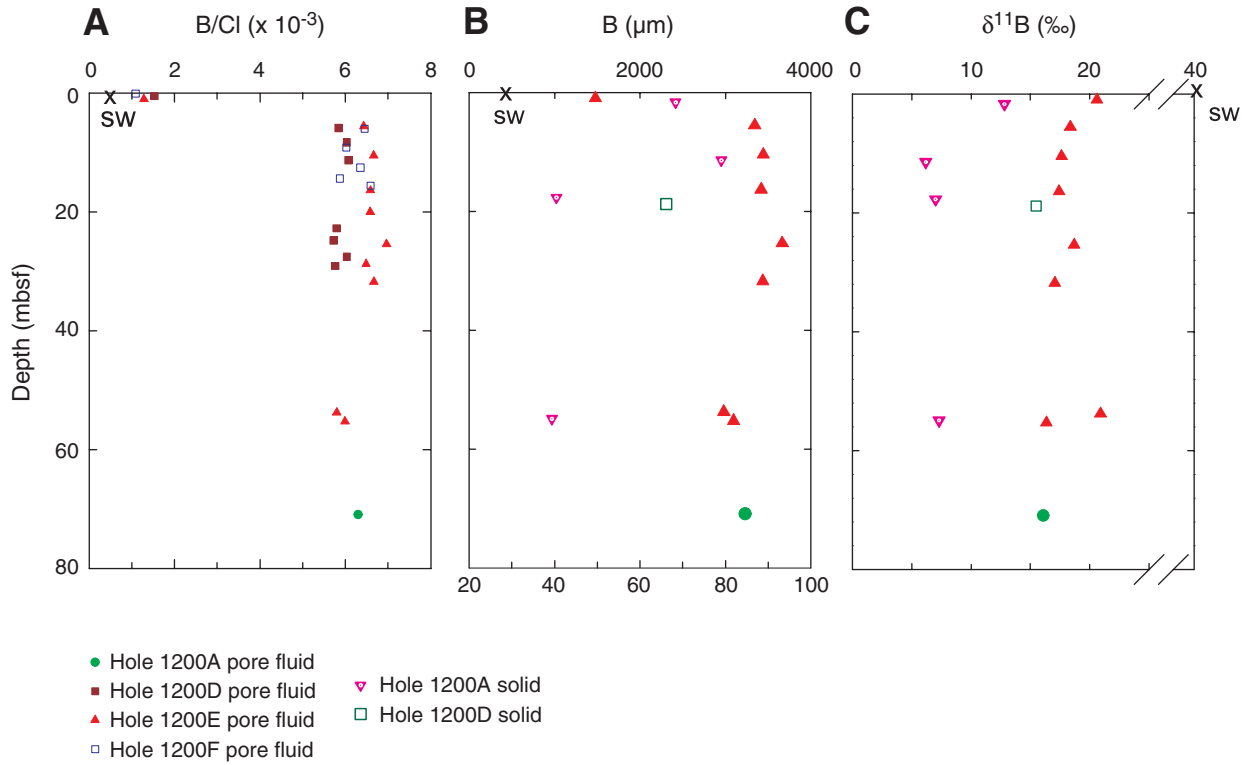
Figure F6. $\delta^{11}B$ vs. 1/B in pore fluids. SW= International Association for the Physical Sciences of the Ocean seawater.
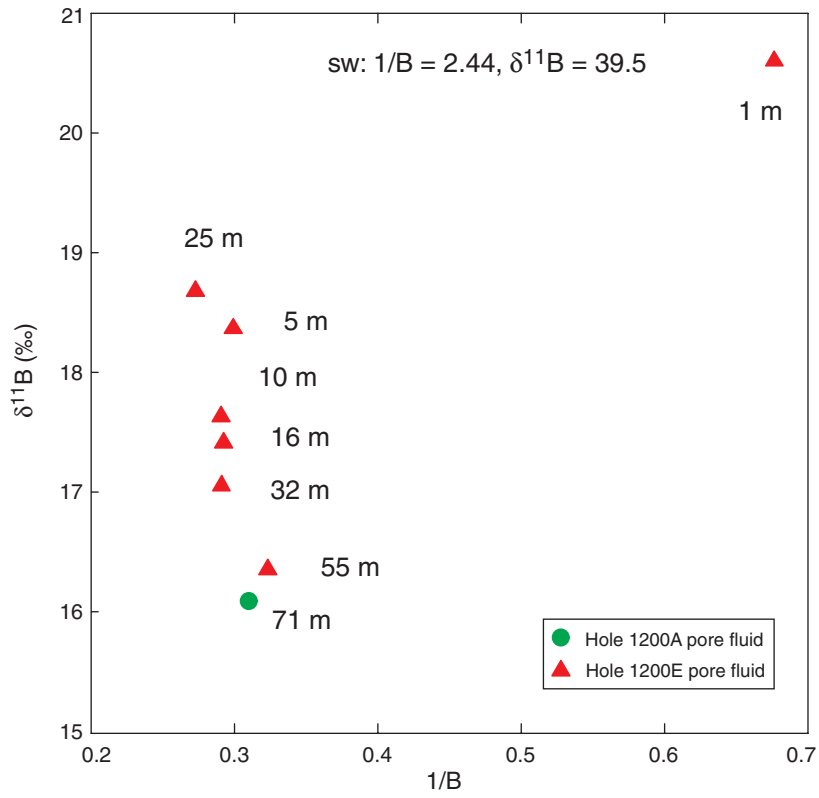
Figure F7. Cl, F, and S concentration-depth profiles in solids.
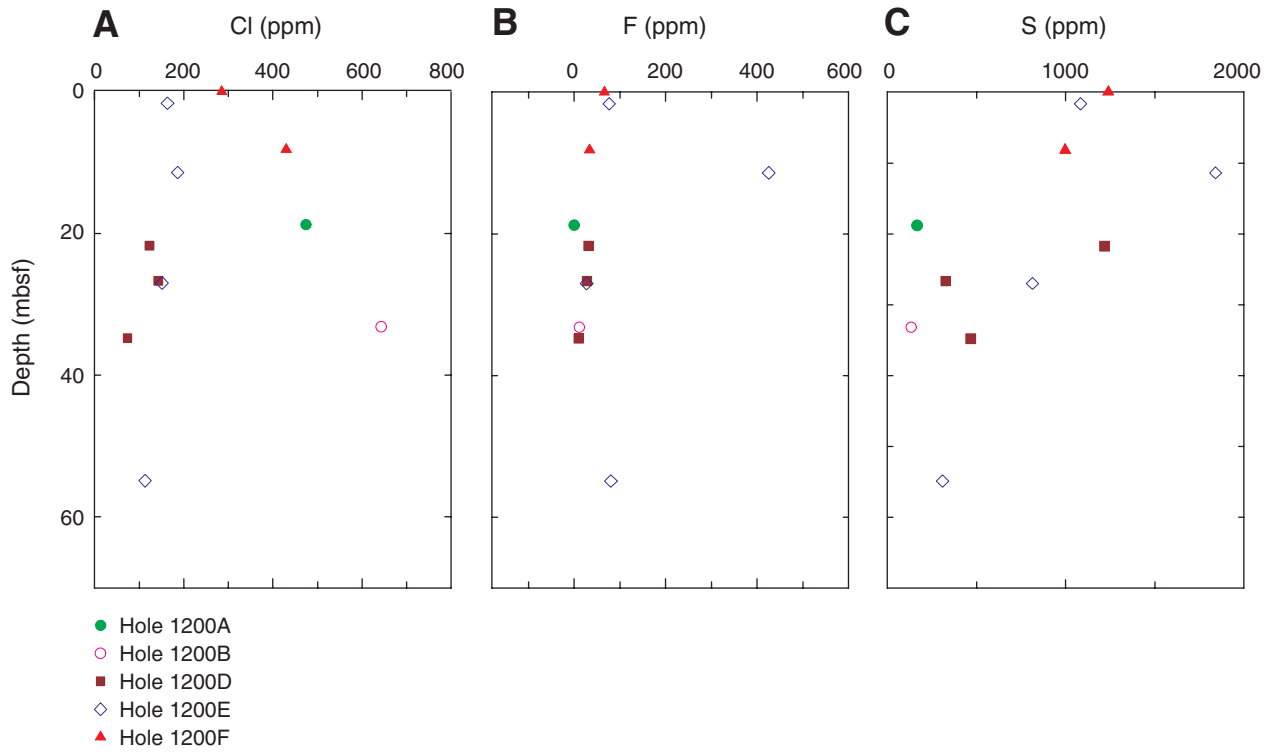
Table T1. Chemistry of pore fluids.

Core, section, interval (cm)	Depth (mbsf)	pH	Cl* (mM)	SO$_4$* (mM)	F* (µM)	SO$_4$† (mM)	F† (µM)	Br† (µM)	δ^{11}B† (‰)	B† (µM)
Method:				IC	ISE	IC	IC	IC		
Seawater:		8.3	540.2	27.94		28.9	68.0	792.3	39.5 ± 0.05	416
195-1200A-										
9R-1, 48–55	70.92	12.5	512.6	28.33	47.4	26.8	81.0	734.1	16.1 ± 0.03	3228
195-1200D-										
1H-1, 40–50	0.45	8.4	540.2	24.38	50.9	25.3	55.9	829.4		
1H-4, 130–140	5.85	11.9	527.3	14.09	11.0	14.0	10.1	785.4		
2H-1, 130–140	8.25	12.0	526.7	17.98	15.0	17.9	15.3	787.6		
3H-1, 130–140	11.25	12.1	531.0	25.11	18.1	25.0	17.5	797.2		
6H-1, 115–126	22.71	12.1	526.7	24.68	28.4	24.5	30.4	768.2		
7H-1, 120–130	24.75	12.4	525.2	26.10	34.7	26.2	38.0	765.0		
8H-2, 97–107	27.52	12.4	521.8	25.14	41.2	23.8	40.5	760.5		
9H-1, 100–110	29.05	12.4	520.1	24.05	44.0	22.7	40.5	757.0		
195-1200E-										
1H-1, 40–50	0.45	8.5	533.5	26.84	60.1	26.2	65.2	819.4		
1H-1, 90–100	0.95	10.3	516.5	4.12	7.1				20.6 ± 0.02	1478
1H-4, 101–111	5.56	12.4	519.4	0.42	73.4	4.8	66.4	724.3	18.4 ± 0.02	3342
2H-3, 130–140	10.45	12.3	516.3	0.22	80.7	2.3	84.7	713.8	17.6 ± 0.03	3443
4H-1, 130–140	13.35	12.2	511.5	0.64	109.7	6.2	111.9	702.3		
4H-3, 130–140	16.35	12.3	518.8	0.87	87.6				17.4 ± 0.04	3419
5H-2, 86–96	19.96	12.3	526.3	1.74	56.0	1.8	50.6	764.1		
6H-1, 124–134	22.49	12.4	523.0	3.75	54.4	3.9	48.6	769.1		
6H-3, 119–129	25.38	12.4	526.0	16.99	57.6				18.7 ± 0.05	3665
7H-2, 130–140	28.75	12.4	522.8	22.36	56.2	22.1	66.4	757.3		
7H-4, 130–140	31.75	12.5	515.4	21.31	48.7	21.4	61.0	731.8	17.1 ± 0.06	3438
10H-2, 130–140	55.25	12.4	516.5	23.05	46.0	23.8	60.7	728.9	16.4 ± 0.02	3094
195-1200F-										
1H-1, 0–10	0.05	8.2	539.0	27.58	49.6	26.0	40.5	812.7		
1H-2, 140–150	2.95	12.2	519.4	8.19	77.0	6.5	83.1	730.7		
1H-4, 140–150	5.95	12.4	514.3	14.55	80.3	13.6	91.1	716.7		
2H-1, 140–150	9.15	12.4	510.9	7.18	65.9	6.9	81.4	710.4		
2H-3, 90–100	11.65	12.4	511.0	9.22	72.3	8.5	76.8	715.0		
3H-1, 140–150	14.35	12.3	510.0	3.27	59.8	2.5	76.3	704.7		
3H-2, 111–121	15.56	12.5	513.0	8.75	76.0	7.2	73.6	715.0		

Notes: * = shipboard data, † = shore-based data. IC = ion chromatography, ISE = ion selective electrode.

Table T2. Mineralogy and chemical composition of bulk solids.

Core, section, interval (cm)	Depth (mbsf)	Lithology	Major minerals	Minor and trace minerals	F (ppm)	Cl (ppm)	SO$_4$ (ppm)	δ^{11}B (‰)	B (ppm)
195-1200A-									
3R-1, 60–75	18.80	Highly altered igneous basement rock	Serpentine, brucite	Chlorite	0	475	167	15.5 ± 0.03	66.18
195-1200B-									
2W-2, 100–115	33.20	Partially altered igneous basement rock	Serpentine, orthopyroxene	Brucite, clinopyroxene, forsterite	11	643	133		
195-1200D-									
6H-1, 23–33	21.73	Serpentine muds	Serpentine	Chlorite, amphibole	31	123	1218		
8H-2, 18–28	26.68	Serpentine muds	Serpentine	Chlorite	28	143	328		
10H-1, 0–10	34.80	Serpentine muds	Serpentine, calcite	Chlorite	9	74	468		
195-1200E-									
1H-2, 15–25	1.65	Serpentine muds	Serpentine, brucite	Chlorite, amphibole	77	164	1084	12.8 ± 0.04	68.33
3H-1, 40–50	11.40	Serpentine muds	Serpentine, aragonite	Amphibole, clinopyroxene	425	186	1841	6.2 ± 0.02	79
5H-1, 12–22	17.72	Serpentine muds	Serpentine	Amphibole	37	200	1077		
7H-1, 110–120	27.00	Serpentine muds	Serpentine	Amphibole, orthopyroxene	27	151	814	7.0 ± 0.05	40.39
10H-2, 100–110	54.90	Serpentine muds	Serpentine	Amphibole	80	113	309	7.3 ± 0.06	39.37
195-1200F-									
2H-1, 0–10	0.00	Serpentine muds	Serpentine	Chlorite, talc, amphibole	66	285	1239		
3H-1, 50–60	8.20	Serpentine muds	Serpentine	Chlorite, talc	34	429	997		